951360

Source Identification Using Acoustic Array Techniques

Susan Dumbacher and Jason Blough
University of Cincinnati

Darren Hallman and Percy Wang
Purdue Univ.

ABSTRACT

Acoustic array techniques are presented as alternatives to intensity measurements for source identification in automotive and industrial environments. With an understanding of the advantages and limitations described here for each of the available methods, a technique which is best suited to the application at hand may be selected. The basic theory of array procedures for Nearfield Acoustical Holography, temporal array techniques, and an Inverse Frequency Response Function technique is given. Implementation for various applications is discussed. Experimental evaluation is provided for tire noise identification.

INTRODUCTION

In the automotive industry, identification of noise sources is necessary to evaluate and reduce noise levels. As alternatives to intensity measurements, acoustic array techniques are currently being evaluated. Often, when a method is found to provide useful information for one test object in one environment, an attempt is made to apply it in situations where it is not necessarily advantageous. Unfortunately, there does not appear to be a single method of source identification that is easy, quick and accurate for all applications. The purpose of this paper is to provide an understanding of the underlying assumptions, advantages and limitations of various acoustic array techniques. Each specific test object and its environment may then be assessed and the most useful technique selected.

In the past, noise source identification has primarily been done by scanning the test object with an intensity probe to measure intensity and sound power. Intensity scans provide valuable information, but are costly for simultaneous acquisition of intensity data at many points, and time consuming for scanning many points sequentially with a single intensity probe. The test time may be reduced at a cost comparable to intensity measurement hardware by obtaining a large amount of spatial data from an array of microphones. This also eliminates the need for human or robot involvement during operation of the test object. The acoustic pressure measurements from the array may be processed using a number of available techniques to provide an estimate of the location and magnitude of acoustic sources. In the automotive industry, such an estimate is useful for identifying airborne and structure-borne sources such as wind noise, tire noise, panel vibration, accessory noise contributions on an engine dynamometer, and passby noise source localization. The array techniques evaluated in this paper include Nearfield Acoustical Holography (NAH), temporal array methods, and an Inverse Frequency Response Function (IFRF) Method. NAH employs a 2-dimensional Fourier Transform to compute a 3-dimensional acoustic field inferred from 2-dimensional pressure measurements. Temporal array methods sum an array of microphone signals which have been shifted with appropriate source-to-microphone time delays. The IFRF technique reconstructs operating source inputs at discrete locations using the FRFs pre-measured by acoustically exciting at those locations. Each acoustic array technique has advantages and limitations which best suit it to particular applications. No one technique is best for all operating test conditions and each method may be modified or further developed. In the following sections, the basic theory of each method is outlined, the advantages and limitations inherent in implementation are discussed, and experimental test cases are provided to indicate possible applications.

BASIC THEORY

In this section, the basic theory of the methods is outlined. The assumptions which are made in the formulations of the system models are indicated. An understanding of these assumptions is important in order to apply the methods to their advantage. The main equations used by each method are also presented, with more complete mathematical derivations given in the references cited.

NEARFIELD ACOUSTICAL HOLOGRAPHY – NAH is based on a spatial transformation of the complex sound

pressure field measured on a two-dimensional surface. Analytical wave propagation theory is used to project the measured pressure distribution to other surfaces in the spatial transform, or wavenumber domain. By successive projections of the measured pressure to parallel surfaces, a three-dimensional map of the acoustic field may be obtained.

NAH was originally developed to locate acoustic sources of interest radiating into a free-field environment [1]. The assumptions inherent in the original theory are that the sources lie on a defined 2-dimensional surface and radiate into a source-free, reflection-free acoustic medium. The measured pressure is used as a boundary condition to solve the homogeneous acoustic wave equation in the region exterior to the sources. The solution to the wave equation for the pressure, *P*, at any point *r* exterior to the measurement surface can be expressed as

P(r) = \int_S P(r') G_D (r-r') dS

where the Green's function, G_D, has a form particular to the geometry of the boundary surface, and *S* is the measurement surface located at *r'*. The Green's function describes the manner in which waves are propagated from the sources, in terms of both the phase shift and amplitude decay undergone with distance from the source surface, and must be derived from analytical wave propagation theory. Since EQ (1) is an integral equation in the form of a convolution, NAH uses computationally efficient wavenumber transform techniques to evaluate it. In simple geometries, such as planar and cylindrical, this procedure is equivalent to performing a two-dimensional FT, which may be implemented efficiently via the FFT. Additionally, it is only in those simple geometries that an analytical solution for the Green's function or its FT can easily be determined. Once the integral in EQ (1) has been evaluated in the wavenumber domain, an inverse FT to the spatial domain is performed to obtain the projected pressure distribution on any surface above the source surface.

The acoustic particle velocity, *U*, is needed to determine intensity or sound power. It may also be calculated on arbitrary planes above the source surface. This is done by expressing the acoustic particle velocity vector in terms of the pressure gradient,

U = {{-j} \over {\rho_0 \omega }} \nabla P .

where ρ_o is the density of the acoustic medium and ω is the frequency of interest. This calculation is also performed in the wavenumber domain, where the spatial derivative may be evaluated by a simple multiplication, and inverse transformed into the spatial domain. The pressure and acoustic particle velocity distributions thus obtained may be projected to the source surface in order to determine the surface vibration and structural acoustic coupling properties. Once the projected pressure distributions and acoustic particle velocity have been calculated based on the measured pressures, the second order quantities of the acoustic field, such as intensity, may be determined.

The previous theory was based on the assumption of sources radiating into a reflection free environment. The NAH theory has also been developed to account for a variety of reflecting surfaces in the region exterior to the source. A method that allows for waves reflected from a surface in the path of the normal component of an acoustic wave, such as the ceiling of an enclosure, has been developed. The method is based on pressure measurements made on two parallel surfaces in the nearfield of the source [2][3][4]. The two surfaces of pressure measurements are used to distinguish the waves travelling away from the source from the waves bouncing off of the reflecting surface and travelling back toward the source. Green's functions of opposite propagation directions, toward the source and away from the source, are applied to each wave type separately. The pressure distributions on a given plane are then expressed as a sum of the incoming and outgoing waves. NAH techniques have also been developed to allow for reflections from the walls of a duct, if the walls are nearly perfectly reflecting and perpendicular to the measurement surface [5]. The measured pressure is extended into an infinite series of image sources which account for reflections from the walls, and the images are propagated along with the measured pressure. These procedures have been combined to develop an NAH method applicable in fully enclosed spaces [6]. The assumptions are that the enclosed walls be acoustically hard and perpendicular to the measurement plane, and that reconstructions can be performed only on planes parallel to the measurement grid (and hence the source surface) which do not pass through the ceiling.

NAH is applicable to sound fields generated by a number of coherent or incoherent sources. If all the data is acquired simultaneously, stationary reference microphones are not needed to phase-reference the array. However, for sound fields generated by stationary, random sources, spatially-fixed reference microphones are useful for averaging the operating data and reducing background noise. If the data is acquired in a number of scans, or if an averaged estimate of the operating data is desired, then reference microphones are required to relate the phase of the pressure recorded during separate scans in a consistent manner. The number and placement of the reference microphones should be chosen such that the reference signals are coherent with the source signals. In this way, noise that is not coherent with the sources is averaged out of the data. To process the data acquired using references, the sound field is represented in terms of a set of fully coherent, mutually incoherent partial fields on the measurement plane. The partial fields can by computed using either the virtual coherence method [7] or the partial coherence method [8]. The multiple coherence may be calculated in order to determine whether a sufficient number and placement of references have been used to fully characterize the sound field. Extra references may also be included to remove unwanted noise sources [9].

Some examples of practical applications of NAH can be found in the literature [10] where NAH techniques were used to locate sources in the interior of a cabin of a small sport utility vehicle, and to locate sources on an idling engine radiating into a semi-anechoic chamber.

TEMPORAL ARRAY TECHNIQUES – Temporal array methods are signal enhancement techniques based on the time delays between suspected source locations and measurement locations. The time delays, or phase shifts, are calculated by assuming a specific source radiation pattern propagating at the speed of sound and measuring the path distances between the source points and the set of measurement locations. The

operating acoustic signals from the array are corrected for the corresponding time delays or phase shifts, and the signals are summed. The resulting summation thus enhances suspected source locations from which a signal emanates, and attenuates source locations from which no signal emanates. The enhancement is provided by the constructive interference between the corrected signals, which occurs only at a true source location. The attenuation is provided by the destructive interference between the signals summed at a location for which no source is present. In the latter case, it is assumed that if no true source is present at a suspected location, the corrected phases for each measurement point calculated at that location will take on a random character, and will thus sum to zero. In practice, this requires that a sufficient number of measurement points are used such that their sum approaches zero near a location where no source is present.

Two methods for determining the location of acoustic sources based on temporal techniques have been applied in this paper. The first method is a time domain method [11][12] in which the cross-correlation functions measured from microphone pairs in an array are shifted by the appropriate time delays, for each suspected source location, and summed. The peaks occurring in the cross-correlations will sum constructively at source locations, and will average out at other locations. A source probability function (*SPF*) at a suspected source location r_o can be constructed by summing the contribution of the cross-correlation function, $R_{ij}(\tau)$, from each microphone pair (*i*,*j*) at the source location. This is expressed as

SPF (r_0) = \sum_{ij} R_{ij} ({{| r_{j} | - | r_{i}| } \over c })

where r_i is the distance between the source location and microphone *i*, r_j is the distance between the source location and microphone *j*, and *c* is the speed of sound. The *SPF* is mapped over a surface to indicate the location of sources on that surface. EQ (3) does not take into consideration amplitude decay with distance from the source, which is equivalent to assuming that the acoustic field is generated by sources radiating planar waves at the speed of sound. Spherically propagating monopole sources may be modelled by including an amplitude decay factor of *1/r* in EQ (3).

The second temporal array method is a frequency domain method [13][14] in which the pressure at the source location at a single frequency is determined by phase correcting in the frequency domain the pressure at each measurement location to account for the time delay. Assuming a point source radiating spherically and propagating at the speed of sound, the sound pressure at the source location r_o is given by

P_{r_0} (f) = {{\sum_i P_{r_i} (f) e^{ j k r_i}} \over {\sum_i 1 / r_i}}

where r_i is the distance between the source location and measurement location *i*, and $k=2\pi f/c$ is the wavenumber at the frequency *f*. The function is mapped over a surface, with regions of high pressure corresponding to source locations. Since the simple monopole model of the pressure assumed in this method is only applicable in the farfield of the source, measurements of the pressure must consequently be made in the farfield. This method yields an estimate of the pressure magnitude at the source.

A practical application of temporal array methods, in which they are applied to find passby noise sources on a high-speed train, can be found in the literature [14].

INVERSE FREQUENCY RESPONSE FUNCTION TECHNIQUE – The IFRF method is a solution technique which is not limited to acoustic systems, but is applicable to all linear systems. In this method, the acoustic system is treated as a system of inputs (source locations) and outputs (measurement locations) passed through a linear filter (the acoustic path) which is described by a set of Frequency Response Functions (FRFs) between the inputs and outputs. The sources of the acoustic field, and hence the strength of the inputs, are then determined by inversion of the measured set of system equations. Since the system FRFs are measured experimentally, they include any reverberant paths between the source and the measurement locations and thus model the environment more accurately than the other methods. However, this method also tends to produce false results if significant errors occur in the measured model of the system, due to error amplification in the inversion process. Much work has been done in the area of indirect force identification applied to structural vibration, with some of the later references cited [15][16][17][18].

The IFRF method is based on measuring the path information, in which time delays and reverberations are inherent, between the selected source locations and the microphones in the array. Using this path information, the array is "calibrated" so that a multiplication with the operating outputs of the array yields source information. The method uses the FRF relationship between inputs to a system, $\boldsymbol{F}(\omega)$, and outputs of the system, $\boldsymbol{X}(\omega)$, via

{\bfm X}(\omega) = [H(\omega)] {\bfm F}(\omega) .

Since EQ (5) is typically an overdetermined set of equations, the inputs can be determined using the pseudo-inverse solution

{\bfm F}(\omega) = [H(\omega)]^+ {\bfm X}(\omega) .

$[H(\omega)]$ is determined prior to operation by applying known inputs to the suspected source locations and measuring the inputs and responses. Once the calibration $[H(\omega)]^+$ of the array is obtained, it is postmultiplied by the operating responses to yield the operating system inputs.

For the application of noise source identification, $\boldsymbol{X}(\omega)$ is the vector of complex pressures from the microphone array and $\boldsymbol{F}(\omega)$ is the vector of source acoustic quantities. The known acoustic inputs can be calibrated to yield the desired source quantities such as pressures and volume velocity. If monopole sources are assumed, sound power and intensity may be obtained from the volume velocity. Non-averaged pressure spectra may be processed directly using EQ (6). This is equivalent to processing transient data. For steady state cases, averaged operating data may be processed for an estimate of the source inputs in the following manner. EQ (5) is postmultiplied by its complex conjugate transpose, or Hermitian, to yield the cross-spectral output matrix of the array, $[S_{yy}(\omega)]$

[S_{yy}(\omega)]={\bfm X}(\omega){\bfm X}^H(\omega) = [H(\omega)] {\bfm F}(\omega) {\bfm F}^H(\omega) [H^H(\omega)] .

$[S_{yy}(\omega)]$ is then experimentally measured in addition to the FRF matrix $[H(\omega)]$. The term $\boldsymbol{F}(\omega)\boldsymbol{F}^H(\omega)$ is the input cross-spectral matrix, $[S_{xx}(\omega)]$, which is to be determined. A pseudo-inverse solution of EQ (7) gives

[S_{xx}(\omega)]= [H(\omega)]^+ [S_{yy}(\omega)] [H^H(\omega)]^+ .

$[S_{xx}(\omega)]$ is an mxm matrix where m is the number of inputs. Its diagonal terms are autopowers, which determine the strength of the discrete sources. Its off-diagonal terms are cross-powers, which determine the degree of correlation between the discrete sources. Taking the square root of the diagonal terms gives an indication of the source strength at the selected locations.

IMPLEMENTATION

The purpose of this section is to provide insight into some of the issues which arise when attempting to implement the acoustic array techniques. The advantages and limitations of the methods are further discussed as they relate to practical application.

NAH – Since NAH is based on analytical wave propagation theory, it is applicable to any source type in any radiating environment. However, it is only computationally efficient to apply the technique to sound fields generated in the simple environments for which the wavenumber distribution of the pressure can be determined by a Fourier Transform, and the analytical form of the Green's function or its FT are known. The geometries of the source and measurement surfaces for which that efficient implementation can be performed exactly are thus limited to simple 2-dimensional surfaces such as planes and cylinders. If the assumption that the sources lie on a defined 2-dimensional surface is violated, the acoustical quantities at the measurement surface are still valid. These quantities can be accurately projected into the farfield and also towards the source surface, until a source is encountered. However, it may be that they cannot be accurately projected onto the source surface for source identification. This is because diffraction from the irregularities in the surface are not accounted for in the Green's function model for a regular surface and may, therefore, yield spurious results for source identification purposes. NAH will compute the sources lying on the regular 2-dimensional surface that would yield the equivalent pressure measurements. More exact methods for irregular surfaces which employ boundary element methods similar to NAH may be formulated, but at a considerable computational disadvantage (on the order of hours rather than seconds).

Theoretically, the spatial resolution with NAH is infinitesimal, since a complete description of the sound field is obtained using EQ (1). The practical spatial resolution is related to the placement of the array and the spacing of the microphones. Measurements must be made in the nearfield of the source in order to obtain the sub-wavelength resolution necessary for a high resolution image of the source. If nearfield measurements are not possible, farfield acoustic holography techniques are available, differing from NAH in the lack of high resolution. The microphones of an NAH grid must be spaced evenly in a given direction in order to employ the 2-dimensional FT. The spacing distance is chosen to avoid spatial aliasing of the sound field, which could occur due to discretization of the measurement surface quantities. As a rule of thumb, measuring at a height above the source which is 1-2 times the spatial sampling interval produces an unaliased image of the sound field with a resolution equal to the spatial sampling interval [1]. As compared to the other acoustic array techniques evaluated in this paper, NAH requires a much larger number of microphone positions for high resolution, and thus more computation time.

Transient data may be processed using NAH. The pressure data is calculated across the whole frequency spectrum at each point, and an inverse FT is performed to the time domain. The result is the spatial distribution of the acoustic data at each discrete point in time. In order to obtain consistent data, either all the data must be acquired simultaneously, or the data must be acquired using a trigger from a repeatable transient signal exciting the structure.

The results from the NAH technique are acoustic field imaging maps. Since NAH is based on an exact solution of the wave equation, the measured pressure can be used to construct 3-dimensional maps of the pressure, velocity, and active and reactive intensity fields. The 3-dimensional maps are useful in a number of ways. They identify radiation points at a source surface and provide insight into the vibrational properties of the surface generating the acoustic field. They indicate the amount of noise detectable at remote locations and the way the energy is propagated from the vibrating surface, through the acoustic medium, and to the remote locations. Maps of the active acoustic intensity in free-fields and the reactive acoustic intensity in lightly-damped enclosures have been especially useful for the latter purpose, as well as for detecting the surface locations which are significant generators of acoustic energy in the field. An estimate of the sound power generated by a source may be obtained by summing the active acoustic intensity over the source surface.

TEMPORAL ARRAY TECHNIQUES – The source assumptions of temporal array methods are as follows. First, all of the suspected source points must be chosen, and the path distances between the source points and the microphones measured. A simple geometrical model of the sound field is assumed, in which the source is approximated as a discrete array of monopoles on a surface concurrent with the source surface. The sources are assumed to radiate into a free-field, and only farfield source information is assumed to be of interest.

Both of the temporal array techniques assume that the sources propagate into a free-field environment. If reflected paths of equal time delay or phase shift exist, “ghost images” of the actual source occur in the reconstructed image. These ghost images give an “apparent location” to the source of the reflection which may coincide with a suspected source location. In that case, a suspected source location may appear as a source when in fact it is not. How a reflected path can cause a non-unique source location, and thus a ghost image, is illustrated as follows. It is well known in geometrical acoustics that a reflecting surface may be replaced by an image source. It is possible for the path lengths, and thus the

corresponding phase shifts, between the measurement locations and the image source to be equivalent to the paths between the measurement locations and a point on the reconstruction surface. By correcting the phase to account for the path distance between several measurement locations and summing those measurements, noise and ghost images are typically averaged out of the data. To ensure this, a sufficient number of source locations and a particular array geometry is chosen [12][14]. Ghost images may be also suppressed by using more measurement locations to formulate the reconstruction. This decreases the probability that a sum of reflected paths will have a consistent apparent location when all the measurement points are summed.

For the time domain temporal array method, a circular arrangement of diametrically opposed microphone pairs is suggested [12]. The circular geometry is chosen because its configuration reduces ghost images. For each microphone pair, the possible source locations lie on a hyperbola, resulting in a non-unique source location. Over short distances, the hyperbola appears as a line. By using multiple microphone pairs, the source locations are determined uniquely by the intersections of these lines. With a circular configuration, the lines emanate from the source location radially. As a result, the overlap between the hyperbolas, caused by leakage, is reduced as much as possible. The microphones forming a pair are chosen opposite one another to increase the distance between them, so that the time delay between the two microphones is not essentially zero. Using the cross-correlation functions between microphone pairs is equivalent to using a number of references so that coherence between distinct sources is not required. With this method, the suspected sources should be located anywhere within the cylindrical volume formed by extending the circular array. In reality, the sources could lie outside the cylindrical volume, and the *SPF* constructed in an exterior region. However, the non-uniqueness of the source locations would possibly result in ghost images which obscure the sources. The solution is to increase the number of microphones. The larger the number of microphones, the lower the probability that non-unique paths will result.

For the frequency domain temporal array method, arrangements which spread the microphones out uniformly in all directions, such as concentric circles, are best at suppressing ghost images. Since temporal array measurements are made in the farfield of the sources, the microphones must be amply spaced to be able to detect the difference in time delays between each measurement point and each suspected source location. One recommendation [14] is to space the measurement locations by a half-wavelength at the center frequency of the frequency band of interest, and to place the array no more than a few wavelengths from the source. These considerations, along with the number of measurement points, will fix the spatial extent of the array necessary to ensure accurate reconstructions.

For the time domain method, all frequencies are used in the calculations, so the maximum source resolution limit is equal to the speed of sound divided by the sampling frequency, or a half-wavelength of the maximum frequency. It should be noted that increasing the maximum frequency beyond the frequency range of the radiating sources will not improve the resolution. It may be possible to increase the resolution by normalizing the cross-correlation function [12]. However, the normalization process removes the information pertaining to the pressure magnitudes of the sources. The frequency domain method is limited to a spatial resolution of a half-wavelength of the frequency chosen. This limitation is due to considering only acoustic radiation with a wavelength characteristic to the specific frequency in the model of the sound field. The half-wavelength resolution is poor at low frequencies or when the spatial size of the source is on the order of the acoustic wavelength. However, the technique can provide useful information with a limited number of microphones and limited computations at higher frequencies where the wavelength is small compared to the source dimensions.

IFRF TECHNIQUE – The discrete suspected source locations must be known prior to the IFRF technique, and acoustic inputs must be applied at each of the locations with the same directivity as the sources, in order to calibrate the array. This may render the method impractical for certain applications. In quality control testing, where source locations are known and magnitudes of the sources can be easily checked to determine whether or not the noise level is acceptable, the IFRF technique may be particularly attractive.

In order for this method to be implemented for noise source identification successfully, the FRF matrix $[H(\omega)]$ used to calibrate the array must be accurately measured. There are several factors to consider. The responses measured at the grid must be due only to the applied inputs. The validity of this is indicated by the coherence functions. If a number of lightly damped modes are present in the environment, the excitation method should be chosen such that leakage does not occur at the peaks. These modes are actually present in the path, and should not be measured inaccurately or computationally removed with smoothing or averaging. With a periodic excitation, leakage does not occur. As a result, a pseudo-random excitation, or specifically a random signal containing energy only at the spectral lines and repeated for each time block, is suggested. The applied source inputs must radiate a sufficient amount of noise to be detected by the microphone array in the presence of background noise, which implies the signal-to-noise ratio must be high enough to yield responses coherent with the measured inputs. If the array is placed at a distance from the source such that time delays are significant, then either the response channels should contain a trigger delay to account for this, or pseudo-random excitation should be used. For the latter case, each measured response time block is due to exactly the same input signal, so the time-delay does not reduce the coherence. The matrix $[H(\omega)]$ must also be well-conditioned. The pseudo-inverse may be obtained using a singular value decomposition, but if the matrix $[H(\omega)]$ is ill-conditioned, the calculated inputs may be mathematically correct – i.e., satisfy EQ (5) – but may not be the actual inputs applied to the system.

The advantages of this method include the following. It is not limited in the frequency content of the radiating sources. The source resolution can be as fine as desired, since it depends only upon the locations selected as suspected sources. The method handles any geometry of the sources or microphone array in any reverberant or non-reverberant

environment. Since the array is calibrated prior to operation, the on-line processing requires only multiplication. These advantages allow an array to be placed directly in the operating environment and calibrated under those conditions.

The use of arrayed microphones and data averaging reduce the effects of noise present in the environment. However, the method is sensitive to inputs coherent with the responses which are not accounted for in EQ (5). If the operating data contains unaccounted for noise inputs, $\boldsymbol{F}_{no}(\omega)$, the reconstructed sources $\boldsymbol{F}\hat{}(\omega)$ will have the form

\hat{\bfm F}(\omega) = {\bfm F}(\omega) + [H(\omega)]^+[H_{no}(\omega)] {\bfm F}_{no}(\omega) ,

where $[H_{no}(\omega)]$ is the FRF matrix between the noise inputs $\boldsymbol{F}_{no}(\omega)$ and the microphone array. The second term in EQ (9) is the error in the reconstructed source inputs. This error term is basically the noise input which is passed through a "filter" of $[H(\omega)]^{+}[H_{no}(\omega)]$. The effect of the noise input on the source reconstruction then depends on the behavior of the "filter", or on how dominant the noise input is in the path information. If the location of the noise inputs are known, they may be treated as sources, and their effects essentially filtered out of the data of interest. For an extremely noisy industrial environment, the array may be placed such that it encloses the test object with acoustic shielding, or the test area itself may be partitioned with shielding.

The results of the IFRF technique are acoustic source quantities at the selected locations. As a result, this method does not lend itself well to source visualization maps, unless a large number of source locations is chosen. Since the experimental FRFs must be measured due to each input, that may be impractical. Analytical FRFs may be used to produce source visualization maps, but may be computationally equivalent to boundary element methods for anything other than free-field environments and planar surfaces.

EXPERIMENTAL RESULTS

In order to test the acoustic array methods in a practical setting, each was applied to the measurement of exterior road noise radiating from a tire. This application is not a direct comparison of the methods, since each method has advantages and limitations best suiting it to particular conditions, but is rather a presentation of the factors involved in experimentally testing each acoustic array method. Acoustic holography based on farfield measurements, an acoustic array technique not evaluated in this paper, has also been applied to identify tire noise [19].

The road noise was created by a 1990 Isuzu Impulse running on a chassis dynamometer. The excitation was provided by driving one front roller on the chassis dynamometer, thus driving one of the front tires of the vehicle.

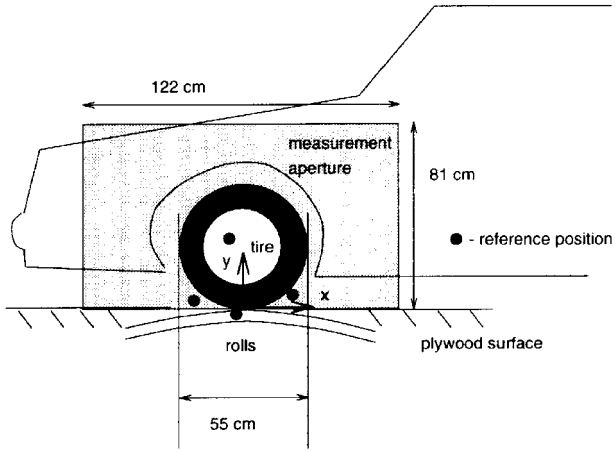

Figure 1: **Schematic of the experimental setup for NAH tire noise test.**

The car was placed in neutral without the vehicle engine running so that no load except rolling resistance was placed on the roller. The roller was outfitted with rough surfacing material to simulate a random road surface excitation and thus widen the frequency spectrum of the excitation. The tire was driven at an approximate speed of 30 km/hr. The chassis dynamometer was turned off between tests and the speed was not measured precisely, so that the actual rotation speed during each test was slightly different. As a result, the same prominent features were observed in the frequency spectrum for each case, but the frequencies at which they occurred shifted slightly. The methods for measuring the noise generated by the tire and dynamometer, using the different acoustic array techniques, are presented in the proceeding sections.

It is important to note that in the experimental tests, the actual locations of the noise sources are unknown. The presented results are only estimations, and may include errors due to violations of the assumptions made in the techniques. Thus, it would be useful to scan the tire area with an intensity probe in order to obtain intensity measurements for comparison.

NAH – A schematic of the experimental setup used in the NAH test is shown in Figure 1. The measurement setup consisted of both the reference microphone system and the measurement array. The environment was assumed to be essentially free-field, so only one plane of measurement data was acquired. Four reference B&K 4130™ microphones were placed in the positions shown in Figure 1 and were used to characterize the total sound field on the measurement plane. A partial coherence method was used to determine the contributions of the independent sound fields on the measurement plane associated with each reference microphone. The measurement array consisted of a vertical line array of 16 PCB Acousticel™ microphones spaced 5 cm apart in the vertical direction and located 5 cm from the tire face. The line array was traversed over 32 horizontal positions with a uniform spacing of 3.8 cm in the horizontal direction, comprising a 32x16 measurement plane of the dimensions and location shown in Figure 1. The entire measurement procedure took about 1 ¾ hours and was evenly divided

between acquisition time and time spent manually incrementing the array horizontally. An automated system for incrementing the array, or the use of more microphones in the array, could be expected to cut the acquisition time in half. Cross-spectral information is needed to perform the partial coherence decomposition of the pressure on the measurement plane. This cross-spectral data was collected with an HP3565™ system, using the LMS FMON™ data acquisition package, at 512 spectral lines over a frequency band from DC to 2048 Hz. 100 averages were used to estimate the cross-spectra. The data was then decomposed and projected back to the source plane using a set of NAH programs written in Matlab™ on a Sun™ workstation. Once the data was collected, the NAH processing of the data took about one minute for each reconstruction surface at each frequency.

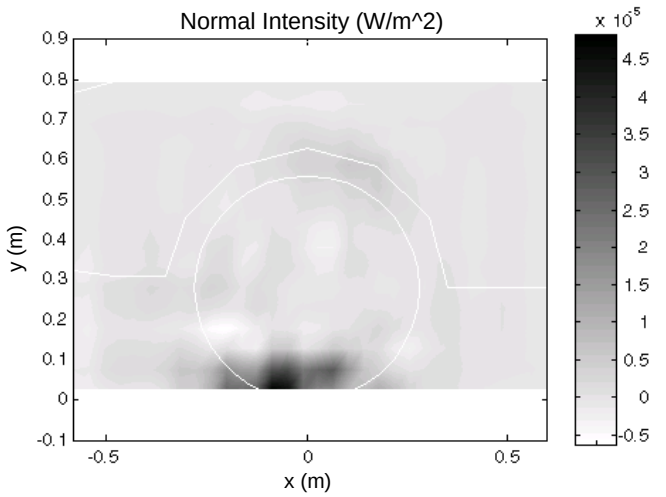

Figure 2: **Normal Intensity on tire surface at 616 Hz as reconstructed by NAH.**

A typical NAH reconstruction result is shown in Figure 2. The normal active intensity on the tire surface is shown at 616 Hz, which corresponded to the first harmonic of the tire tread rotation frequency. At this frequency, most of the acoustic energy is generated from the center of the contact patch. The sub-wavelength resolution capability of NAH is also observed. At 616 Hz, the acoustic wavelength is 55 cm, but the source of the tire noise is resolved to a patch of about a 5 cm radius.

Figure 3 shows the normal intensity at 1088 Hz on the tire surface, reconstructed from the pressure measured on the grid surface. Most of the noise comes from two spatially separated sources at the center and in front of the contact patch, the one in front being dominant at this frequency. Although they are separated by less than a wavelength, NAH can still resolve them independently.

There are several factors pertaining to identifying tire noise sources which utilize the advantages of NAH. The most obvious is the surface geometries of the test object and the test environment. The face of the tire is essentially a plane, and acoustic shielding was placed to render the chassis dynamometer test chamber a free-field environment. Although NAH is applicable to enclosed spaces, one of the assumptions is that the "walls" of the space be hard and perpendicular, which is violated if odd-shaped objects are present as reflectors in the environment. Other factors include the relatively small distance between the located sources and the small dimension of the sources compared to the acoustic wavelength. These are not restrictions with the high spatial source resolution capability of NAH.

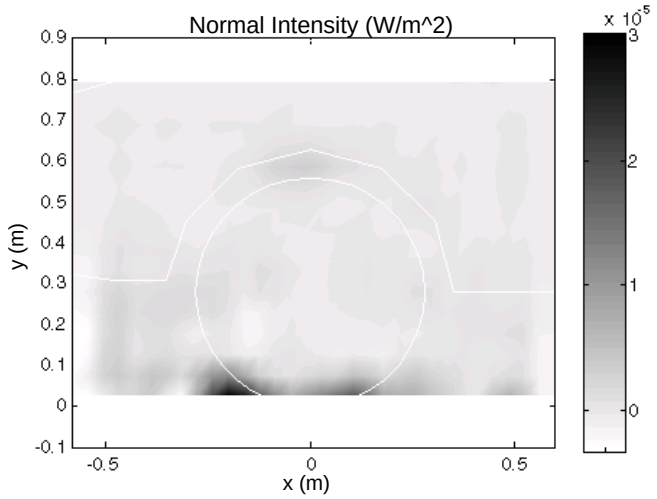

Figure 3: **Normal Intensity on tire surface at 1088 Hz as reconstructed by NAH.**

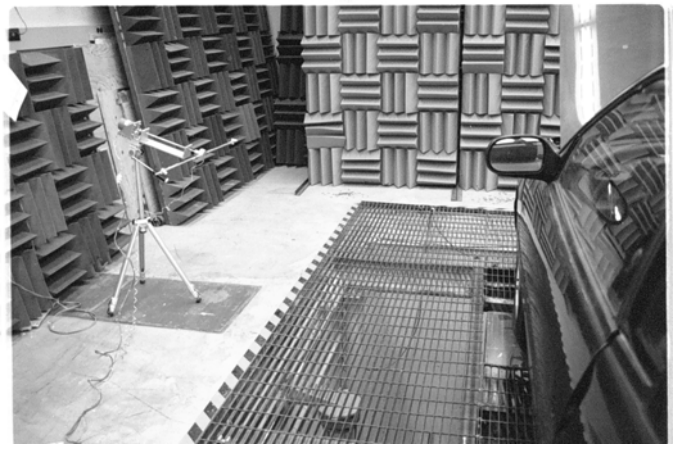

Figure 4: **Photograph of time domain temporal array setup using circular array.**

TEMPORAL ARRAY METHODS – A photograph of the experimental setup for the time domain temporal array test is shown in Figure 4. A measurement apparatus was constructed with an automatically incrementing arm containing two microphones on either end, spaced 80 cm apart. The arm was incremented in 18^o intervals for a total of 10 microphone pair locations in the circular array. The summation of 10 signals at the cross-correlation peaks results in a 20 dB amplification of a source signal above a noise floor, which was felt to be sufficient. Using 30 microphone pairs would have given a 29.5 dB amplification. The array was placed in a plane parallel to the tire at a distance of 1.44 m from the tire, and was tilted 20^o towards the tire in order to ensure that the suspected sources (located at the contact patch) lay within the cylindrical volume of the circular array

previously mentioned. The 10 cross-correlation functions between the diametrically-opposed microphone pairs were obtained using an HP35650™ data acquisition system with LMS FMON™. The time data was sampled at a rate of 16384 Hz for 16384 samples for a time block of 1 second. In retrospect, the sampling frequency could have been reduced to yield an equivalent resolution, since the maximum source frequency was well below 8192 Hz. Also, since only the peaks in the cross-correlations corresponding to the time delays were summed, the time block could have been reduced from one second to the 20 or 30 ms containing the minimum and maximum time delays. To increase the maximum time delay, and hence use more time points in the calculations, the distance between the microphone pairs could be increased. However, there is a practical limit to the microphone spacing, at which point the distance between the microphones and the source becomes too large. 100 averages were used to estimate the cross-correlation functions, comprising a total data acquisition time of about 30 minutes, including the 10 incrementations. The cross-correlation data was processed using a Matlab™ program, which calculated the *SPF* map from the cross-correlation functions in a few seconds. The cross-correlation functions were not normalized, and planar wave propagation was assumed.

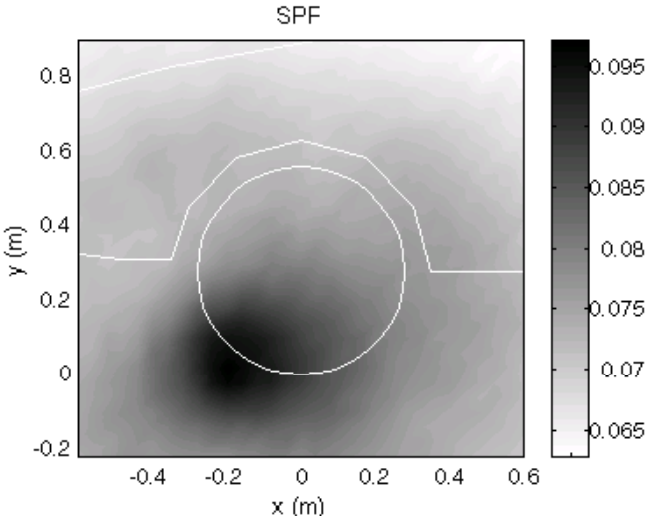

Figure 5: ***SPF* reconstructed on the tire surface using the time domain temporal array method.**

Since this method is performed in the time domain, the result is the summation of the source locations over all frequencies. The result for the *SPF* on the tire surface is shown in Figure 5. Most of the noise is generated from the front and center of the contact patch, as seen in the previous NAH methods. However, since all frequencies are included in the reconstruction, the sources are blurred together to generate a frequency independent estimation of the overall source. This problem may be overcome by Fourier Transforming the cross-correlation function into the frequency domain and band-passing certain frequencies, then inverse transforming back into the time domain. However, the narrow-band data collected would have a much higher correlation in time, thus possibly obscuring the source locations. The resolution using this method appears to be about 10 cm in either direction, which is about five times the expected value of 2 cm, thus indicating that over all frequencies, the source is a distributed one.

There are several factors pertaining to identifying tire noise sources which affect the applicability of the time domain temporal array method. This technique has the ability to visualize the locations of the overall sound sources with a limited amount of data (only 10 microphone pairs, as compared to 16x32 microphones in the NAH test) and with a fair degree of spatial resolution. However, if source information is desired at a particular frequency, this method may not provide the necessary information.

Figure 6: **Photograph of the experimental setup used in the frequency domain temporal array method.**

A photograph of the frequency domain temporal array setup is shown in Figure 6. The array was outfitted with three concentric circles of diameters 24 cm, 72 cm, and 120 cm, respectively, each containing 8 microphones spaced at 45^{o} intervals. This arrangement suppresses the formation of ghost images, which occur using this method due to non-unique solutions for the source location at a single frequency. The data was collected as single time records at each microphone, from which an estimate of the pressure frequency spectra was obtained. This is equivalent to analyzing transient data. To provide a more accurate estimate of the spectra, a separate set of averaged FRF data, with one microphone in the array chosen as a reference, was also collected. This requires steady state operating conditions. Using the FRF data, the absolute pressure and phase at each microphone location was found by multiplying the FRF associated with that microphone by the square root of the reference microphone auto-spectrum. Both the time and FRF data sets contained 2048 spectral lines over a frequency range from DC to 2048 Hz. 100 averages were used to estimate the FRF data. The estimate of the reconstructed pressure was found to be within 10% at each measurement location for both methods of obtaining the pressure spectra. Since the transient time data took only one second to collect, it was used. The time data was transferred to a Sun™ workstation, Fourier Transformed, and then used to reconstruct the pressure on the tire surface. The reconstruction process took about 1 minute for each frequency.

A typical result for the mean-square pressure reconstruction on the tire surface at 644 Hz, which was the first harmonic of the tread pattern rotation frequency, is shown in Figure 7. It is clear that the primary source is the contact patch, where the pressure is highest. However, the resolution using this method is poor because the acoustic wavelength at this frequency is comparable to the dimensions of the source (i.e., the tire). The resolution improves with increasing frequency, as witnessed in the reconstruction of the pressure on the tire surface at 1091 Hz, shown in Figure 8. In this case, the source of the noise is concentrated at the front end of the contact patch, which agrees with the results from the NAH analysis. However, the two sources which were resolved at this frequency using NAH are indistinguishable using this method, due to the half-wavelength resolution limit.

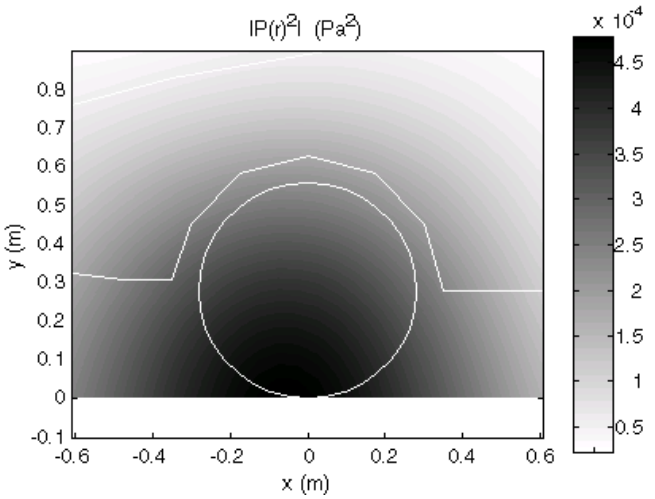

Figure 7: **Pressure reconstructed on the tire surface at 644 Hz using the frequency domain temporal array method.**

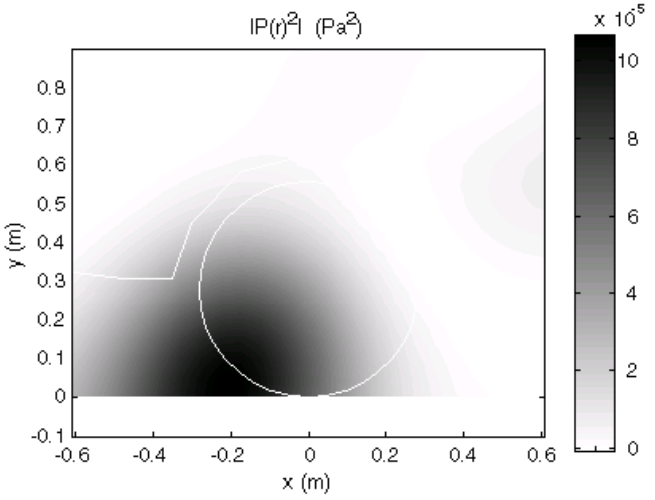

Figure 8: **Pressure reconstructed on the tire surface at 1091 Hz using the frequency domain temporal array method.**

There are several factors pertaining to identifying tire noise sources which affect the applicability of the frequency domain temporal array method. The most limiting factor is the poor degree of spatial resolution at and below the frequencies with wavelengths comparable to the source dimensions. This method would yield much more useful information if the higher frequencies, where nearfield measurement requirements may become a limitation for NAH, were of interest. Also, it was possible with NAH to make nearfield measurements of the tire. If only farfield measurements were possible or practical, the temporal array methods would be applicable. Inversely, the arrays must be in the farfield, so if only nearfield measurements were possible, temporal arrays would not be applicable. Another factor is the limited amount of data used in this test (only 24 microphones, as compared to 16x32 microphones in the NAH test). Having a larger amount of spatial data is definitely an advantage in averaging out noise which is not coherent with the source signals, but also requires more computational effort.

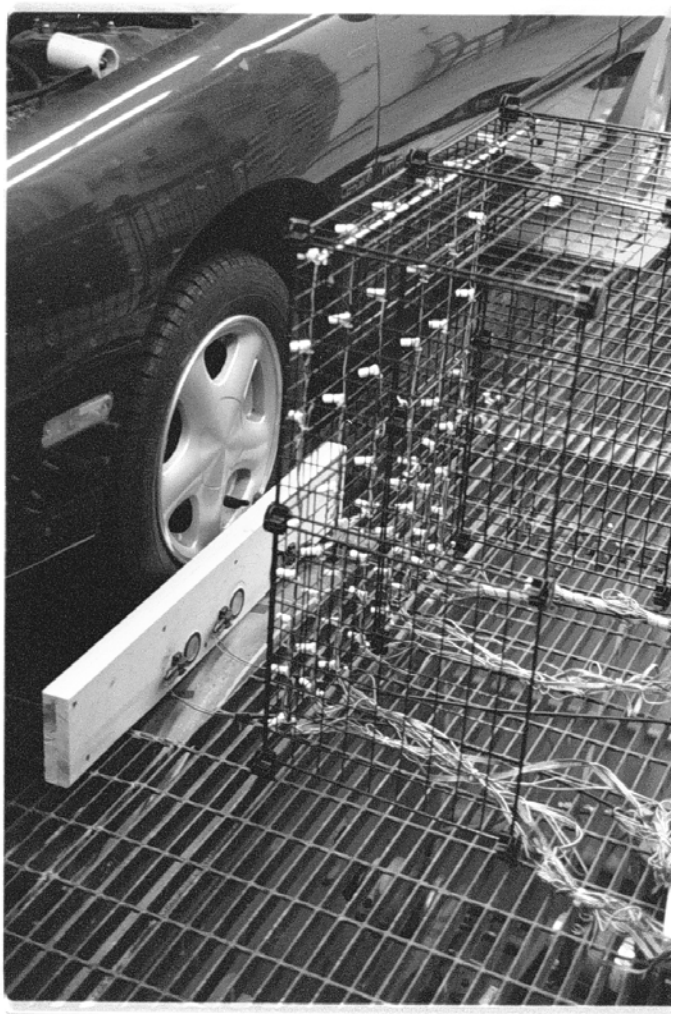

Figure 9: **Experimental test setup for the IFRF technique.**

IFRF METHOD – Photographs of the experimental setup for the IFRF technique are shown in Figure 9. A 61 cm by 71 cm array, with a total of 56 microphones, was placed 18 cm from the tire. The microphones were not evenly spaced, but were placed with a higher concentration near the bottom half of the tire. The array was "calibrated" by driving 4 cm diameter piezoelectric exciters, mounted in a board containing cavities, with pseudo-random noise and measuring the FRFs. The six exciter locations were 15 cm apart at the front, center,

and rear contact patches of the tire, at heights of 3.8 cm and 26.8 cm. The three exciters located at a height of 3.8 cm were chosen to correspond to the sources located using the NAH technique. There were many lightly damped acoustic modes present, so by using pseudo-random excitation, the leakage at the resonances was minimized. The FRFs were acquired at 1024 spectral lines from 288 to 1310 Hz with 50 averages using HP3565™ data acquisition hardware and LMS-FMON™ software. The total FRF acquisition time was on the order of minutes. The piezoelectric exciters were calibrated for acoustic input quantities in an anechoic chamber. Volume velocity per voltage input to the exciters was obtained using farfield pressure measurements from three microphones for averaging, while pressures per voltage input to the exciters were obtained by placing microphones directly in front of the exciters. The exciter calibration setup is given in Figure 10. The particular exciters used only radiate a sufficient amount of energy at frequencies above 500 Hz, so the array calibration data is only valid above 500 Hz.

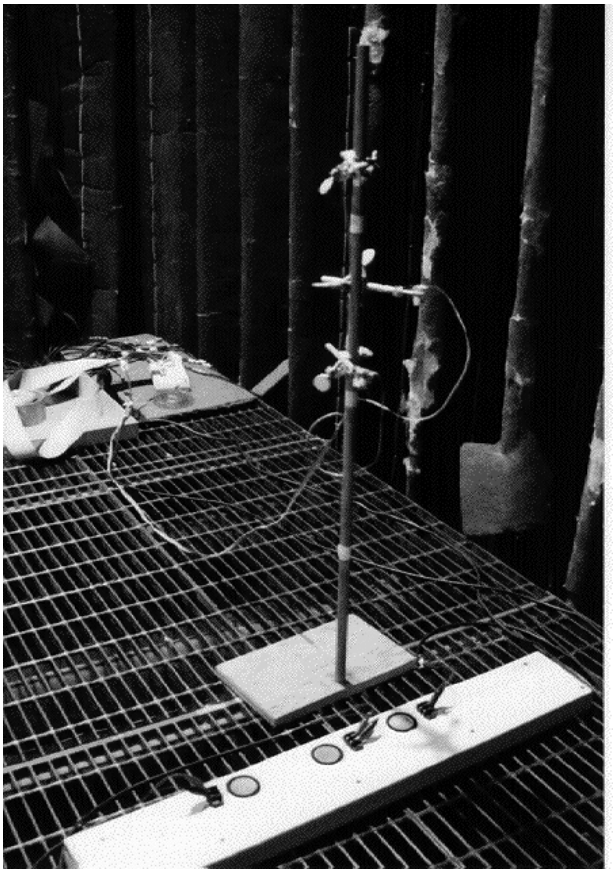

Figure 10: Volume velocity calibration of the piezoelectric exciter inputs used for the IFRF technique.

The operating data was taken as a transient set of pressure spectra from the 56 microphones. The frequency range was 288 to 1310 Hz with 1024 spectral lines. The data was transferred to an HP700™ workstation and processed using algorithms executed in Matlab™. Processing time was on the order of a few seconds for each frequency.

The volume velocity source results at 680 Hz, the first harmonic of the tread pattern rotation frequency, are given in Figure 11. Since only six source locations were chosen, the magnitudes are displayed as bar charts. Most of the noise is generated from the center of the contact patch. The volume velocity source results at 1108 Hz, equivalent to the 1088 Hz data using NAH, are given in Figure 12. Most of the noise is generated from the front of the contact patch. The IFRF technique results agree with those of NAH.

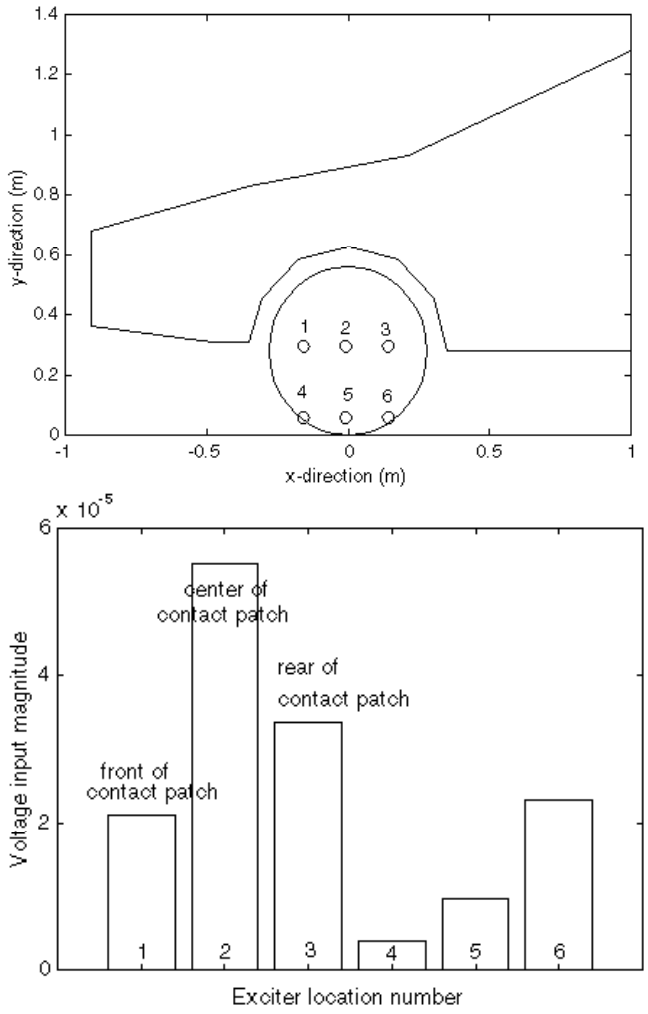

Figure 11: **Source volume velocity reconstructed on the tire surface at 680 Hz using the IFRF technique.**

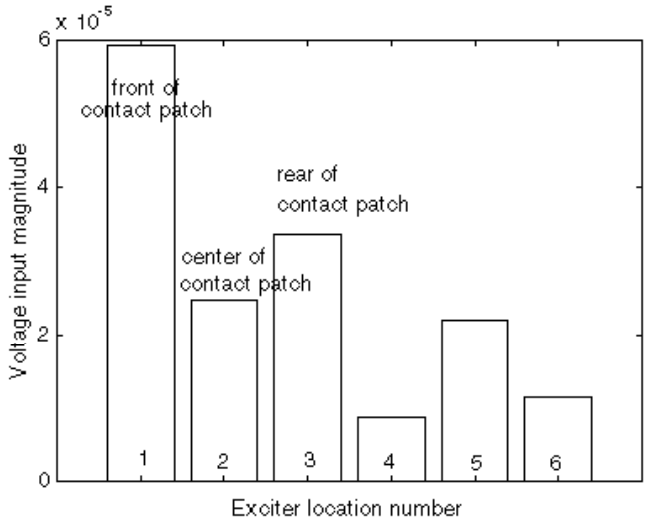

Figure 12: **Source volume velocity reconstructed on the tire surface at 1108 Hz using the IFRF technique.**

There are several factors pertaining to identifying tire noise sources which affect the applicability of the IFRF method. The most obvious is that the actual locations of the tire noise sources were not known, but were assumed to be at the locations found using NAH. A larger number of input locations could have been chosen to verify that those were the dominant source locations. Using a larger number of inputs would also allow for a map-type result for visualization purposes. Also, since the source surface of the tire was planar and the environment essentially free-field, this application did not take advantage of the two strong points of the IFRF method, mainly its validity with any source geometry and any reverberant environment. However, results consistent with the two previous methods for the source locations were obtained.

CONCLUSIONS

Several acoustic array techniques have been presented as alternatives to intensity measurements for noise source identification. The techniques evaluated include NAH (a spatial transformation method), time and frequency domain temporal array methods (signal enhancement techniques), and an IFRF method (a solution technique). Each of the methods has advantages and limitations which render it ideal for certain applications. A summary of the practical aspects involved in application is given for each of the techniques in Table 1. To provide experimental application, each of the methods was applied to tire noise identification. The actual noise source magnitudes and locations were unknown for this case.

REFERENCES

(1) J.D. Maynard, E.G. Williams, and Y. Lee, "**Nearfield Acoustic Holography: I. Theory of Generalized Holography and the Development of NAH**", *J. Acoust. Soc. Am., Vol. 78(4) pp 1395-1413, 1985*.

(2) M. Tamura, "**Spatial Fourier Transform Method of Measuring Reflection Coefficients at Oblique Incidence: I. Theory and Numerical Examples**", *J. Acoust. Soc. Am., Vol. 88(5) pp 2259-2264, 1990*.

(3) Z. Hu and J.S. Bolton, "**The Measurement of Plane-Wave Reflection Coefficients by Using Two-Dimensional Spatial Transforms**", *J. Acoust. Soc. Am., Vol. 88(Suppl. 1) S173, 1990*.

(4) D. Hallman and J.S. Bolton, "**A Technique for Performing Source Identification in a Reflective Environment by Using Nearfield Acoustical Holography**", *Proc. Noise-Con, pp 479-484, 1993.*

(5) M. Villot, G. Chaveriat and J. Roland, "**An Acoustical Holography Technique for Plane Structures Radiating in Enclosed Spaces**", *J. Acoust. Soc. Am., Vol. 91(1) pp 187-195, 1992*.

(6) D. Hallman, J.S. Bolton, L.B. Long, and H. Takata, "**The Application of Nearfield Acoustical Holography to Locate Sources in Enclosed Spaces Exhibiting Acoustic Modal Behavior**", *Proc. of the 12th International Modal Analysis Conference, pp 1076-1082, 1994*.

(7) J. Hald, "**STSF - a unique technique for scan-based Nearfield Acoustical Holography without restrictions on coherence**", *B&K Technical Review, 1988*.

(8) D.L. Hallman and J.S. Bolton, "**Multi-Reference Nearfield Acoustical Holography**", *Proc. Internoise, Toronto, pp. 1165-1170, 1992*.

(9) K.B. Ginn and J. Hald, "**Engine Noise: Sound Source Location Using the STSF Technique**", *Proc. of the 1993 Noise and Vibration Conference, pp 361-364, Traverse City, Michigan.*

(10) D.L. Hallman, J.S. Bolton, S.M. Dumbacher, D.L. Brown, B.W. Libbey, and M.J. Lally, "**Acoustic Source Location in Vehicle Cabins and Free-field with Nearfield Acoustical Holography via Acoustic Arrays**", *Proc. of the 19th International Seminar on Modal Analysis, Leuven, Belgium, September 1994.*

(11) R. Zimmerman, D.L. Brown, I.E. Morse, "**Cross-correlation analysis for noise source location using microphone arrays**", *Proc. of Internoise, San Francisco, pp 923-930, 1978*.

(12) P.Mas and P. Sas, "**Spatial localisation of sound sources, based on measurements of cross-correlation functions**", *Proc. of 3rd International Conference on Structure-borne and Air-borne Noise and Vibration, Montreal, 1994*.

(13) K. Kido, M. Abe, H. Noto, and Y. Ikegami, "**Sound source detection and location using cross spectra between signals picked up at many points**", *Proc. of Internoise, Edinburgh, pp 1103-1106, 1983*.

(14) Y. Takano, K. Terada, E. Aizawa, A. Iida, and H. Fujita, "**Development of a 2-Dimensional Microphone Array Measurement System for Noise Sources of Fast Moving Vehicles**", *Proc. of Internoise, Toronto, pp 1175-1179, 1992.*

(15) T.J. Roggenkamp, "**An Investigation of the Indirect Measurement of Broadband Force Spectra**", *PhD Dissertation, Purdue University, August 1992*.

(16) S.M. Dumbacher, "**Spatial Filtering for Signature Enhancement**", *PhD Dissertation, University of Cincinnati, June 1994*.

(17) W. Hendricx, "**Accurate vehicle FRF measurements for indirect force determination based upon matrix inversion**", *Proc. of the 19th International Seminar on*

Modal Analysis, Leuven, Belgium, pp 1037-1049,September 1994.

(18) P. Mas, K. Wyckaert, P. Sas, "**Indirect force determination based upon impedance matrix inversion: A study on statistical and deterministic accuracy**", *Proc. of the 19th International Seminar on Modal Analysis, Leuven, Belgium, September 1994.*

(19) I. Sakamoto and T. Tanaka, "**Application of Acoustic Holography to Measurement of Noise on an Operating Vehicle**", *International Congress and Exposition, SAE Technical Paper 930199, Detroit, Michigan, March 1993*.

Table 1: **Application requirements for acoustic array techniques.**

	NAH	Time domain temporal	Frequency domain temporal	IFRF
Source				
High frequency	limited by nearfield	yes	yes	yes
Low frequency	yes	limited by farfield	limited by farfield and resolution	limited by lack of modes
High resolution	yes	c/f_s	$\lambda/2$	yes
Planar source surfaces	yes	yes	yes	yes
Odd-shaped source surfaces	no	yes	yes	yes
Unknown specific source locations	yes	yes	yes	no
Environment	yes	yes	yes	yes
Free-field				
Box-shaped reverberant	yes	ghost images	ghost images	yes
Odd-shaped reflectors	no	ghost images	ghost images	yes
High heat in nearfield	limited by microphones	yes	yes	yes
No farfield space	yes	no	no	yes
Data	large number	smaller number	smaller number	smaller number
Measurement points				
Transient	yes	yes	yes	yes
Average	yes	yes	yes	yes
Output	acoustic 3-D maps	SPF maps	pressure maps	discrete source quantities